

APPLIED RESEARCH

5G Non-Terrestrial Networks With OpenAirInterface: An Experimental Study Over GEO Satellites

FLORIAN VÖLK¹, (Graduate Student Member, IEEE), THOMAS SCHLICHTER²,
SUMIT KUMAR³, (Member, IEEE), ROBERT T. SCHWARZ¹, (Member, IEEE),
ANDREAS KNOPP¹, (Senior Member, IEEE), MARWAN HAMMOUDA², THOMAS HEYN²,
JORGE QUEROL³, (Member, IEEE), SYMEON CHATZINOTAS³, (Fellow, IEEE),
AND ADAM KAPOVITS⁴

¹Chair of Signal Processing, University of the Bundeswehr Munich, 85579 Neubiberg, Germany

²Broadband and Broadcast Department, Fraunhofer IIS, 91058 Erlangen, Germany

³Snt-Interdisciplinary Centre for Security, Reliability and Trust, University of Luxembourg, 1855 Luxembourg City, Luxembourg

⁴Eurescom GmbH, 69123 Heidelberg, Germany

Corresponding author: Florian Völk (florian.voelk@unibw.de)

This work was supported in part by European Space Agency's Advanced Research in Telecommunications Systems (ESA ARTES) Advanced Technology Project 5G-GOA, "5G Enabled Ground Segment Technologies Over the Air Demonstrator," European Space Agency (ESA) under Contract 4000133231/21/UK/AL.

ABSTRACT The 3rd Generation Partnership Project (3GPP) aims to integrate non-terrestrial networks (NTNs) with terrestrial 5G networks. In this context, prototyping and testing are essential to demonstrate the readiness of new 5G-NTN releases. However, commercial 5G protocol stack implementations are usually costly and closed solutions, which makes it challenging for universities and nonprofit research institutions to adapt and customize them for 5G-NTN testing and development purposes. Software-defined radio testbeds that utilize open-source software implementations are an attractive alternative. In this article, we describe our protocol stack adaptation of an open-source implementation for 5G-NTN based on OpenAirInterface (OAI), which runs on commodity hardware. We evaluate the performance of our 5G-NTN in various layers in real-world environments with a transparent geostationary satellite. We validate our testbed with a variety of Internet applications. These include streaming video, web browsing, and voice over IP. The results indicate that the current implementation utilizing the 5 MHz bandwidth is reliable over several hours and achieves both downlink and uplink speeds of 3.6 Mb/s while maintaining a typical geostationary latency of approximately 530 ms. The tests demonstrate that our 5G-NTN testbed is a reliable alternative to costly commercial implementations.

INDEX TERMS Satellite communication, 5G mobile communication, radio access networks, space communications.

I. INTRODUCTION

The terrestrial infrastructure of fifth-generation mobile networks (5G) is insufficient to provide seamless connectivity to previously unserved and underserved areas on Earth. In certain areas, deploying 5G base stations is not economically or logistically feasible. Communication satellites have

The associate editor coordinating the review of this manuscript and approving it for publication was Nurul I. Sarkar¹.

evolved to an unprecedented degree and can provide services that require high throughput and bandwidth. Satellites have extensive coverage and are widely available, making them ideal partners for 5G networks. The coverage, resilience, and reliability of 5G networks can be enhanced via satellites, thereby increasing the value of these networks.

In 3rd Generation Partnership Project (3GPP) Release-15 [1] and Release-16 [2], the potential role of communication satellites in complementing a terrestrial network

(TN) was identified. This resulted in a detailed study of deployment scenarios, channel models, frequency ranges, satellite constellations, access modes, footprints, and antenna models. In March 2022, the first specifications for integrating satellites into 5G were finalized [3]. For the first time, satellites were considered outside a transport network, focusing on providing direct access to 5G services at the user terminal. This means that the user terminal connects directly to a ground-based next-generation node B (gNB) via a satellite channel (Figure 1). However, integrating 5G TN and non-terrestrial network (NTN) components is not as straightforward. In 5G new radio (NR) TN protocol stack development, satellite channels were not considered in any early deployment scenarios. As a result, significant adaptations are needed before 5G-NTN-based services can be deployed.

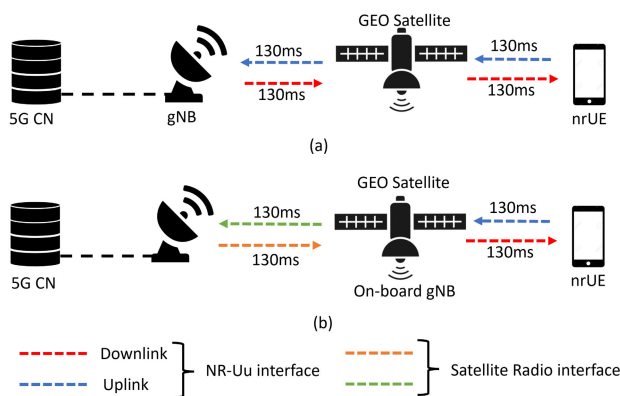


FIGURE 1. High-level 5G-NTN architecture using (a) a transparent-payload geostationary satellite and (b) a regenerative-payload geostationary satellite with on-board gNB. Note that the one-way delay for (a) is ~ 260 ms, whereas that for (b) is ~ 130 ms.

In recent years, academic researchers have developed several proof of concept (PoC) demonstrators for 5G-NTN with support from industry and government space agencies. As 3GPP standardization further optimizes the 5G-NTN in Releases 18 and 19 [4], open research platforms, such as 5G-NTN testbeds, are essential for simplifying the development of standardized prototypes [5]. These testbeds play a vital role in research and standardization by providing a secure and controlled environment for testing and evaluating emerging technologies. These are crucial for the development of future NTN specifications. The testbeds ensure that the new NTN standards are secure, reliable, and cost-effective before deployment.

In this work, we discuss protocol development and provide details on live over-the-satellite experiments performed during one of the pioneer 5G-NTN projects, 5G-GOA [6], and we share the results with the community. To our knowledge, this is the first work that has adapted the 5G-NR TN protocol for geostationary Earth orbit (GEO) satellites and demonstrated a 5G-NTN connection over the satellite.

Adaptations were made in the terrestrial protocol stack of OpenAirInterface (OAI) [7], an open-source software-defined radio (SDR) framework implementing 4G/5G base stations and user terminals, to address the challenges posed by the GEO satellite channel.

We developed a PoC demonstrator for in-lab validation [8] and live experiments over the satellite [9]. Our goal is to evaluate the performance of typical internet applications such as web browsing, voice over IP (VoIP) calls, video streaming, and transport protocols. In this study, we conduct experiments and present our findings. The adapted source code is now available to researchers under the OAI Public License V1.1 [10].

The remainder of this paper is organized as follows: Section II presents the challenges associated with 5G-NR-based NTN. Section III describes the adaptations for GEO satellites in OAI. Section IV and Section V present the measurement setup and outline the assessment and measurement results. In Section VI, we provide future research directions. Finally, we present the conclusions in Section VII.

II. CHALLENGES IN THE 5G-NTN

The implementation of 5G-NTN using GEO satellites is associated with several challenges. In a transparent payload setup, the satellite reflects the incoming ground signal back to the ground after amplifying the signal and converting the frequencies. This configuration makes it easier to deploy 5G-NTN, as existing satellites can be utilized; however, compared with that of regenerative-payload satellites, the round-trip delay (RTD) between the gNB and user equipment (UE) is doubled, as shown in Figure 1 [11]. We considered a transparent-payload GEO satellite in our work, and the challenge is due to the significant distance of the GEO satellite from Earth. This causes the following issues:

- a The RTD between the gNB and UE becomes ~ 520 ms; see Table 1. This breaks all protocols at all layers because the protocols work in a closed-loop fashion. Timers within a closed-loop system are specifically engineered to withstand the maximum delay experienced on Earth's surface. Consequently, adjustments across all the protocol layers are necessary.
- b Another challenge for the 5G-NTN is the high path loss caused by the large distance between the UE and the satellite, especially with GEO satellites orbiting at 35.786 km.

Below, we discuss some of the key challenges caused by the transparent-payload GEO satellite-based 5G-NTN.

A. RANDOM ACCESS

After initial downlink synchronization, an active UE initiates the random access (RA) process [13]. The UE decodes the information transmitted on the broadcast channel by the gNB, sends message-1 (MSG-1) on the physical random access channel (PRACH), and then waits for MSG-2 from the gNB. The time the UE waits is called the random access response

TABLE 1. Typical round-trip delays in terrestrial and non-terrestrial systems [12].

Technology	Height/orbital altitude	Possible cell/beam size	Max. round-trip delays
cellular macro	10 m to 25 m	500 m	0.016 ms
cellular rural	35 m	5 km	0.16 ms
LEO	600 km	50 km to 90 km	~ 26 ms
GEO	35 786 km	120 km	~ 520 ms

(RAR) window. Once it receives MSG-2, it sends MSG-3 to the gNB and waits for MSG-4. This waiting time is called the contention resolution timer (CRT). If the UE does not receive MSG-2 or MSG-4 within a predefined time window, it resends the corresponding message. Figure 2 illustrates the exchange of these messages. When using the same RAR and CRT timeout window as for the TN when deploying the 5G-NTN over GEO satellites, no response is received from the gNB at the UE. Therefore, the RTD must be extended proportionally to the reception time window [2].

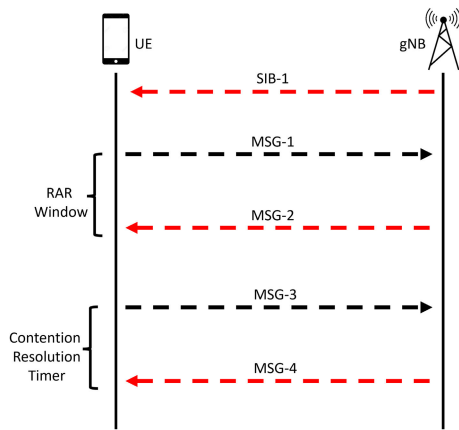


FIGURE 2. Messages exchanged between the UE and gNB during the random access process, along with the associated random access response window and contention resolution timer.

B. HARQ FEEDBACK

The hybrid automatic repeat request (HARQ) is a 5G wireless communication error correction process. HARQ functions as a stop-and-wait protocol, meaning that each parallel HARQ process is assigned a unique ID. The ID can be reused only after the corresponding feedback is received. The TN version of 5G includes 16 HARQ IDs, allowing for 16 parallel transmissions. After transmission, each HARQ ID waits for either acknowledgment (ACK) or no acknowledgment (NACK). However, the time to wait for feedback in a transparent-payload GEO satellite is excessively long, and during this time, a particular HARQ ID will be unavailable. Continuing with the existing protocol stack could result in a scenario in which new data transmission becomes impossible simply because there are no available HARQ process IDs.

This situation, commonly referred to as ‘‘HARQ stalling,’’ as noted in [14], is particularly challenging in a GEO setting because of the very large RTD, which requires an impractical number of HARQ process IDs. Thus, in [2], it was decided to turn off the HARQ feedback so that transmission could continue without the HARQ process needing to wait for the ACK/NACK signal. In such cases, retransmission is either managed by an automatic repeat request (ARQ) within the radio link control (RLC) or entirely delegated to the transport layer protocol, such as in the transmission control protocol (TCP), as indicated in [15].

C. TIMERS, OFFSETS AND BUFFERS

Because of the excessive RTD in the 5G-NTN compared with the TN, the timers and buffers on all the protocol stack layers (medium access control (MAC), RLC, packet data convergence protocol (PDCP), and radio resource control (RRC)) will expire prematurely. In addition, in the gNB, the time-slot difference between the reception and corresponding transmission must be adjusted. This point is discussed below.

1) k_{offset} (MAC)

After receiving downlink control information (DCI) in DL slot n , the slot for the uplink (UL) is PUSCH, which is determined by an offset of k_2 ; thus, the UE transmits in slot $n + k_2$. The current number of values of k_2 (0–32) is not sufficient for the large RTD of the NTN, especially when the timing advance (TA) applied by the UE is also much larger than k_2 [16]. Thus, an additional offset is required to create the entire offset $n + k_2 + k_{offset}$. An illustration of this process is shown in Figure 3. This k_{offset} is part of the timing relationship enhancements and is used for several procedures in the physical layer, for example, extending the RAR and the contention resolution window.

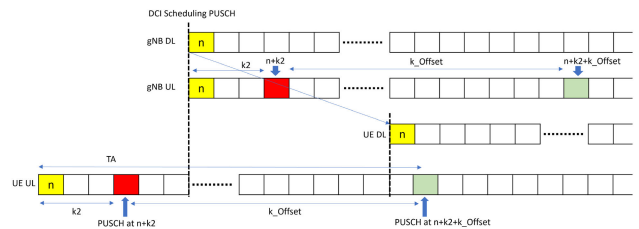


FIGURE 3. Illustration of uplink scheduling with and without k_{offset} [16]. The k_{offset} must be adjusted according to the round-trip delay.

2) t-DiscardTimer (PDCP)

This timer applies to the PDCP entities on the transmitter side. The PDCP entities store the service data unit (SDU) from the upper layer in a transmission buffer and initiate the t-DiscardTimer after transferring it to the RLC. The Timer can be set in the range of 10 ms to 1500 ms or deactivated by setting an infinite duration, as specified in [17]. Once the t-DiscardTimer for a PDCP SDU expires or the successful

delivery of the PDCP SDU is confirmed (via the PDCP status report transmitted by the peer PDCP entity), the transmitting PDCP entity discards the buffered PDCP SDU along with the corresponding PDCP protocol data unit (PDU).

3) t-ReorderingTimer (PDCP)

This timer is applied to the PDCP entities on the receiver side. On the receiver side of an RLC entity in acknowledged mode (AM), the t-ReorderingTimer is used to detect the loss of any RLC PDU in the lower layers.

4) t-ReassemblyTimer (RLC)

This timer is applied to the RLC that receives entities. The RLC that receives entity reassembles PDUs in unacknowledged mode (UM) and AM. This process is crucial for detecting potential loss of RLC PDUs in the lower layers. If the PDUs inside the receive window are not in sequence, the timer t-Reassembly starts and waits for the missing PDU. When the t-Reassembly timer expires, the receiving entity delivers any PDUs containing contiguous packets before or after the sequence gap to the upper layers. The configuration of t-Reassembly allows for fixed values within the range of 0 ms to 200 ms, as outlined in [18].

Table 2 summarizes all the timers and offsets that need to be adjusted.

TABLE 2. Specific 5G-NTN timer/constant adaptations.

Protocol layer	Timers/Constants
MAC	k_{offset} , random access response window, contention resolution timer
RLC	t-Reassembly
PDCP	t-DiscardTimer and t-Reordering

III. ADAPPTIONS IN OPENAIRINTERFACE

In the 5G-GOA project, we modified the protocol stack to address the challenges discussed in Section II. We used the OAI 5G-TN version as the baseline and made significant adjustments [5]. Importantly, we did not modify the air interface. We used the 5G-TN waveform for the air interface in 5G-GOA.

We also introduced several improvements, such as a new graphical user interface (GUI) for OAI based on the QT-GUI. We explicitly modified the OAI physical layer (PHY) and MAC to incorporate the following functionalities: i) support for a 5 MHz bandwidth with a 15 kHz sub-carrier spacing (SCS), ii) integration of multiple bandwidth parts (BWPs), iii) comprehensive frequency division duplex (FDD) scheduling at the MAC layer, facilitating uninterrupted downlink (DL) and UL transmission and reception, iv) improved support for multiple UEs with enhancements for simultaneous RA, and v) an enhanced “disable HARQ” feature to strengthen collaboration with the upper layers, particularly the RLC and PDCP.

A. PHY AND MAC LAYER ADJUSTMENTS

We added a common delay parameter for the TA at the command line. Consequently the RTD is provided as a command line parameter to the UE for initial TA. This command line parameter is important because our gNB does not broadcast serving-satellite ephemeris. Our TA command transmission accounts for a delay equal to or greater than twice the one-way delay between the gNB and UE. This TA command in the MAC control element is transmitted from the gNB to the UE to maintain UL synchronization in the time domain. Consequently the TA periodicity was adjusted so that our UE supports closed loop TA updates in all scenarios.

In addition, we implemented a method in which our UE considers an offset at the start of the RAR window, using the same commandline parameter applied to the TA. This means that the start of RAR window is delayed by an estimate of UE-gNB RTD. The RA procedure, a crucial part of our connection establishment method, required some adaptations to support the simultaneous RA process for more than one UE. During the generation of MSG-1, the UE selects a preamble index randomly by generating a random number. It was necessary to improve this method of preamble selection by generating a random number depending on the current CPU count cycle.

TABLE 3. OpenAirInterface modifications for 5G-NTN during the 5G-GOA project.

Layer	Modifications
PHY	Extension of OpenAirInterface RF-simulator to support simulation of long propagation delays Non-NTN-specific features: - Support of 5 MHz bandwidth (15 kHz subcarrier spacing) - Phase tracking reference symbols - Support for bandwidth parts
MAC	Hybrid automatic repeat request (ARQ) feedback deactivation at gNB and UE Adaptations to support uplink timing advance and random access procedures Frequency division duplex scheduling
RLC	Disabling hybrid ARQ - ARQ interaction Increase ARQ buffer size Increase maximum sequence numbers
PDCP	Increase Discardtimer to the currently maximum allowed value Increase t-Reordering timer to the currently maximum allowed value Increase protocol data unit buffer size Increase maximum sequence numbers
RRC	Timers T300, T301 and T311 are set to the currently maximum allowed value
Misc	New QT based KPI-GUI

As agreed for the 5G NR-NTN in Release 17, we introduced a $k2$ offset value called k_{offset} in our OAI 5G NR-NTN implementation on both the gNB and UE sides, adding this offset to the signaled $k2$ value in the DCI. The k_{offset} value is provided to gNB and UE as command line parameter

and an update of the k_{offset} value is not relevant for our scenario with GEO satellites where the TA update procedure is sufficient. Therefore, our implementation does not allow changing the k_{offset} value after initial access. Moreover, it should be mentioned that in OAI, DL and UL frame timing are aligned at gNB, so k_{mac} was not needed.

B. HIGHER LAYER ADAPPTIONS

Because of the high RTD induced by the 5G-NTN link, we also increased the value of t-DiscardTimer to cover several cumulative maximum durations; without this modification, the timer expires prematurely, resulting in premature discarding of the SDU. In addition, increasing the t-DiscardTimer value increases the buffer size at the transmitter because it has to store the incoming SDUs as well as the SDUs that are still waiting for received receipts. Similarly, for the t-DiscardTimer value, we increased the t-Reordering timer to accommodate the cumulative maximum delays. The RRC configures the t-Reordering timer value, and the maximum duration, as specified in [17], is 3000 ms.

To counteract the latency caused by large RTDs, we increased the value of the t-Reassembly timer. When HARQ is enabled, t-Reassembly should also cover the maximum time allowed for HARQ retransmissions (which may be greater than the RTD). This ensures that the reassembly process considers the HARQ delay, allowing for accurate data reconstruction. The modifications in RLC, PDCP and RRC were sufficient so that modifications in non-access stratum (NAS) were not required.

In OAI gNB and OAI UE, the DL HARQ processes can be either enabled or completely disabled using command line parameters. If HARQ is enabled, the maximum number of HARQ processes is 16, as specified in Release 15 and 16. However, using HARQ for GEO satellite based 5G-NTN is not advisable due to the high additional delay, which leads to ‘‘HARQ stalling.’’ Therefore, we disabled HARQ completely using command line parameters.

We expanded the OAI GUI to display key performance indicators (KPIs) such as block error rate (BLER), achievable throughput, number of scheduled resource block (RB), and modulation and coding scheme (MCS) of the link (Figure 4). Additionally, we created a new version of the RF-simulator to facilitate the experiments without hardware. All enhancements and extensions are integrated into the development branch of OAI [10]. A summary of our changes can be found in Table 3.

IV. MEASUREMENT SETUP

A. HARDWARE AND SOFTWARE SETUP

Our measurement setup included two UEs connected to a gNB. General-purpose x64 computers with a Linux Ubuntu 20.04 LTS operating system ran the 5G-NTN protocol stack for all three network components. The SDRs used were Ettus X310 devices connected to computers via a PCI Express Interface. Additionally, we installed the OAI standalone

architecture (SA) 5G core network (5GC) on the gNB computer.

Figure 5 illustrates the reference architecture for the experimental study, which features a 5G-NR link connecting two OAI UEs and the OAI gNB. All devices were on the ground at a station in Neubiberg, Germany. This location provided the measurement environment for conducting a real over-the-air test of our NTN platform over SES’s ASTRA 2F GEO satellite located at 28.2° East. The satellite created a single NTN cell for our European service zone and facilitated seamless connectivity between the UEs and the gNB.

For transmission in the UL, we utilized a block-upconverter to convert the frequencies from the lower SDR frequency band to the satellite transmission frequencies in the Ku-band. The received satellite signals were then converted to lower SDR frequencies via our low-noise block downconverter. All hardware components were synchronized using the same 10 MHz reference clock to ensure precise operation.

The GEO satellite acted as an analog repeater in space. It received and then retransmitted 5G-NR signals, allowing the air interface between the OAI UE and OAI gNB to be relayed. The hub station features a 7.6 m Ku-band antenna with a 400 W high-power amplifier, which provides an equivalent isotropically radiated power (EIRP) of approximately 85 dBW for saturation and a G/T of 37.7 dB/K. This setup ensured a guaranteed C/N of at least 15 dB for the 5G-NR UL and DL (Figure 6). The bandwidth of each carrier allocated to the 5G-NTN DL and UL was 5 MHz. Figure 6 shows that the local oscillator of the SDRs has not been filtered and is part of the in-band spectrum. The figure shows that the link budget for the test was more than sufficient for QPSK modulation. The focus of the experiment was to evaluate the impact of adjustments to the higher protocol layers and control plane features on performance. Table 4 lists the configuration parameters of the 5G-NTN demonstrator.

TABLE 4. Parameter for over-the-satellite testing.

Parameter	Value
NTN band	Ku-band
Duplex mode	Frequency division duplex
$f_0^{Tx,UL}$	14 040.75 MHz
$f_0^{Tx,DL}$	14 034.75 MHz
Subcarrier spacing	15 kHz
Transmission bandwidth	5 MHz
Fast Fourier transform size	512
Sampling rate	7680 kSps
Round-trip delay	512.15 ms
Satellite terminal type	7.6 m Anchor Station
Modulation scheme	QPSK
Satellite	SES’s ASTRA 2F @ 28.2° East (single beam)
R_{max}	679/1024
OH^{UL}	3/14
OH^{DL}	4/14
$N_{PRB}^{Bw,\mu}$	25
T_S^{μ}	0.000 071 428 571 428 571 43 s

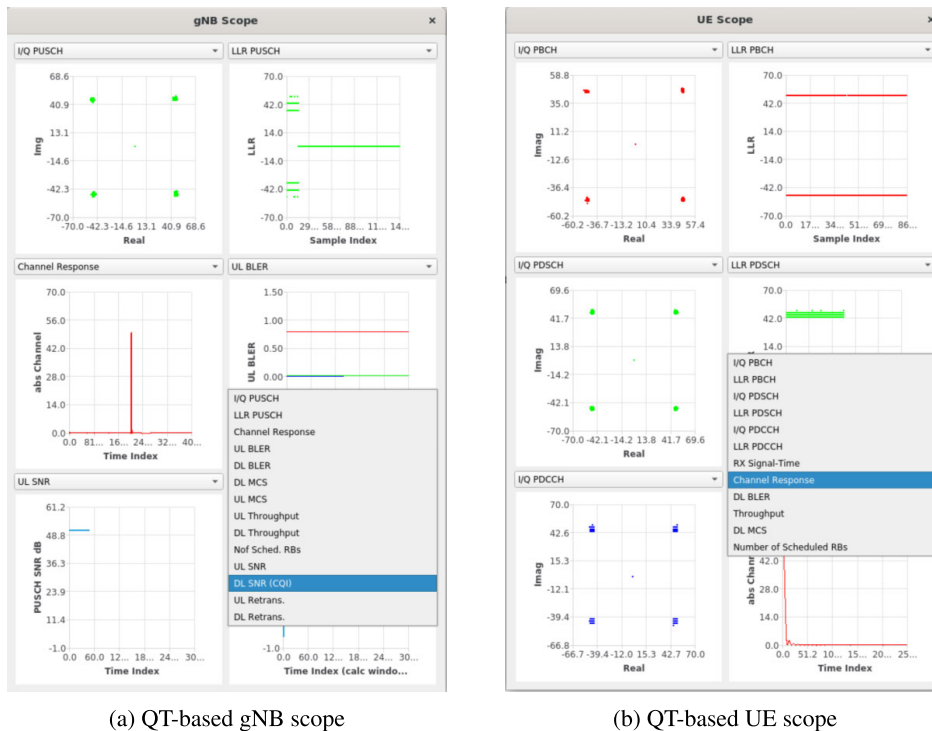


FIGURE 4. QT-based graphical user interface to display key performance indicators (KPIs) for gNB and UE, developed during the 5G-GOA project. It visualizes various KPIs for the uplink and downlink in real time. Users can choose which KPIs they want to display.

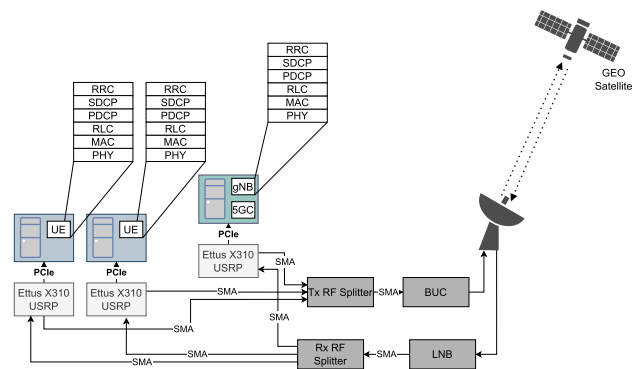


FIGURE 5. Architecture for the field trial. Our demonstrator includes the adapted protocol stack for OpenAirInterface.

B. PERFORMANCE ESTIMATION

We used Equation 1 from TS 38.306 [19] as a baseline to estimate the maximum throughput (TP) for our experiment.

$$TP[bps] = Q_m R_{max} (1 - OH) \frac{N_{PRB}^{Bw, \mu} 12}{T_S^\mu} \quad (1)$$

where Q_m is the maximum supported modulation order, R_{max} is the coding rate, OH is the overhead, μ is the SCS, $N_{PRB}^{Bw, \mu}$ is the maximum RB allocation, and T_S^μ is the average OFDM symbol duration in a subframe. We considered QPSK MCSs with a modulation order of two and only one carrier.

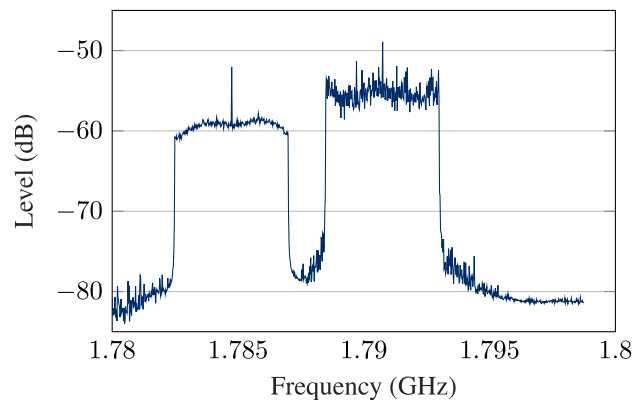


FIGURE 6. Transmitting and receiving satellite spectra from the gNB (left) and UE (right). A local oscillator can be seen in the spectra in both the gNB and the UE.

This means that our TP was affected mainly by R_{max} (Table 5.1.3.1-1 in [19]) and OH for UL and DL, respectively. We used a fixed QPSK MCS for the gNB configuration file. The parameters are listed in Table 4.

V. RESULTS

A. TIMING ADVANCE ESTIMATION

The 3GPP standardization bodies introduced system information broadcast 19 (SIB19) to support the TA estimation of UE with Global Navigation Satellite System

(GNSS) capabilities. However, an interface between the network control center of the satellite network operator for exchanging 5G-NTN parameters was unavailable for our proof-of-concept application. From the satellite network operator itself, we received the precalculated orbit parameters of the satellite in two line element (TLE) format.

TLE data is commonly used to represent a satellite’s orbit. It consists of mean orbital elements that precisely define an object’s location in space with a few kilometers of accuracy. The data is stored as TLE and is used in combination with specific analytical propagation models. The SDP4 Orbit Propagator builds on SGP4 by incorporating solar and lunar gravity. It applies to satellites with an orbital period of 225 minutes or greater. SDP4 makes it possible to estimate the position of a space object within an order of magnitude of one kilometer [20].

We used a self-developed mechanism for the OAI *phy-test mode* to determine the over-the-satellite delay for the TA. The *phy-test mode* is an option in the OAI softmodem. It enables the gNB to consistently schedule the downlink shared channel (DLSCH) and uplink shared channel (ULSCH), even in the absence of a UE. After the initial DL synchronization in the *phy-test mode*, the UE sent ULSCH dummy data with a preconfigured TA offset, which approximately represented the RTD, in slot eight via the PUCCH to the gNB. At the gNB, we observed a substantial time difference. We then manually optimized the TA offset at the UE until we received the dummy data at the correct ULSCH slot at the gNB. After completing this procedure, we used the TA parameter to start the UE and gNB in normal SA mode. We were able to record the tracked TA values in the SA mode over a measurement period of several hours.

Figure 7 shows the estimated (MATLAB SDP4 solver) and tracked TA offsets in SA mode for three measurement periods. The minimum and maximum values were recorded to calculate the delta between the extreme values (Table 5). In addition, Figure 8 shows the absolute error between the estimated TA values based on the TLE files and the real TA values recorded during our measurements, which were automatically adjusted by the gNB after the initial TA configuration. During our measurement process, we realized that the orbit information based on the TLE files had to be more accurate to determine the initial TA value with sufficient accuracy. Therefore, it was necessary to manually optimize the initial TA value whenever the gNB and UE were inactive for a longer period to ensure that the TA error was below 0.01 ms before starting the initial attachment in SA mode.

TABLE 5. Results of timing advance estimation.

	Min (ms)	Max (ms)	Delta (ms)
SDP4	255.962	256.186	0.224
Measurement	255.959	256.180	0.221

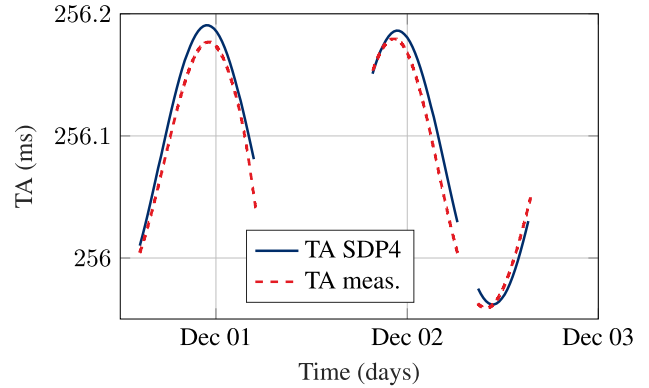


FIGURE 7. Timing advance (TA) estimation is based on the UE position and the estimated satellite position via two line element (TLE) data. The estimated TA value differs from the measured TA value to such an extent that random access was not possible without manual adjustments of the TA value.

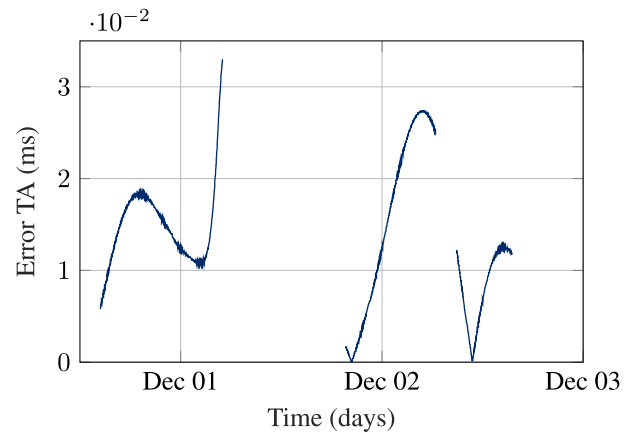


FIGURE 8. Absolute error of the timing advance (TA) estimation. Most of the time, the error was larger than 10^{-2} ms.

B. INITIAL ATTACHMENT

The first step in processing a 5G SA connection is synchronizing the UE with the gNB. This synchronization process includes DL and UL synchronization. DL synchronization occurs first, followed by UL synchronization. Our UE successfully received the DL synchronization signals. Subsequently, the UE completed the RA process using the estimated TA value. After the synchronization process, our UE completed the RRC connection establishment procedure and sent a registration request message to our 5GC for registration. After successful registration with the 5GC, the gNB sent an RRC reconfiguration message to the UE. Finally, the UE completed the establishment of the PDU session and was ready for data transmission through the established PDU session.

C. PERFORMANCE EVALUATION

1) THROUGHPUT

In this study, we used the open-source tool *iperf3*¹ to measure the maximum achievable bandwidth of the user datagram

¹<https://packages.ubuntu.com/focal/iperf3>

protocol (UDP) on our 5G-NTN testbed. We operated our 5G-NTN testbed for MCS scores of 0 to 9. Figure 9 shows the calculated TP for UL and DL based on Equation 1 and the measured TP for UL and DL. We observed that our 5G-NTN testbed achieved the expected TP for all QPSK MCSs. In addition, we analyzed the maximum Goodput (GP) for typical transport protocols (Table 6). Due to the congestion control mechanism, we initially observed slow behavior for the TCP and quick UDP internet connections (Quic). The maximum TCP and QUIC GPs were lower than those of the UDP owing to the additional acknowledgment messages.

TABLE 6. Maximum goodputs of transport protocols.

	UDP	TCP	QUIC
Downlink (Mb/s)	4.00	3.90	3.90
Uplink (Mb/s)	4.45	4.35	4.20

2) NETWORK LATENCY

Figure 10 shows the distribution of network latency measured via the Linux *Ping* command. It also shows the distribution of the times for establishing connections with the Quic protocol, which were measured via *qperf*.² The distribution of the Timing Advance (TA) values, as depicted in Figure 7, is shown in Figure 10 to emphasize the lower threshold for the network latency. It took 20 s to 30 s of additional processing time to achieve a successful ping compared with the TA estimation. We established a successful connection via the Quic protocol within a time frame of 658 s to 670 s. Our results show that the RTDs of our testbed are comparable to the RTDs of commercial GEO satellite internet providers [21], [22].

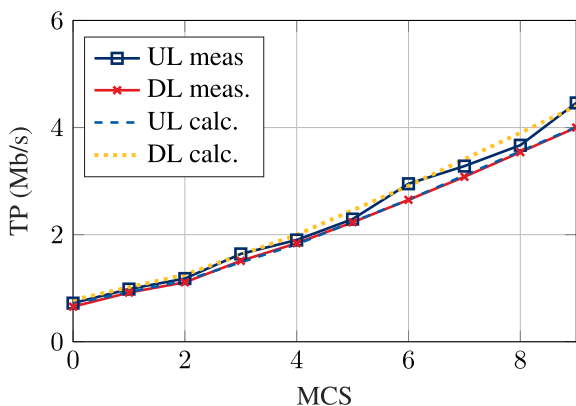


FIGURE 9. Maximum throughput of uplink (UL) and downlink (DL) depending on the modulation and coding scheme. The throughput increases with increasing modulation and coding scheme.

D. VALIDATION OF TWO UES

We determined a measurement sequence for measuring the TCP GP via two UEs. The first UE, UE2, sent a continuous

²<https://github.com/kosekmi/qperf>

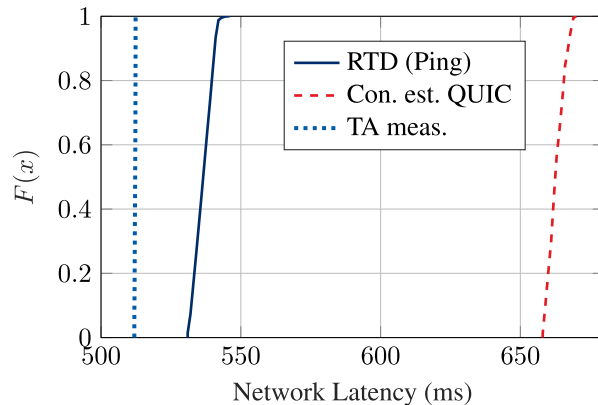


FIGURE 10. The empirical cumulative distribution function (ECDF), denoted as $F(x)$, represents the probability that the network latency assumes values less than or equal to the corresponding abscissa. The values for the time advance (TA) are the lower bound for the network latency. The ping-based round-trip delay (RTD) was within the expected range for geostationary satellites. Quick UDP internet connections (QUIC) were established shortly afterwards.

data stream for 30 s, after which UE1 started sending data for 15 s. The scheduling algorithm ensured that both UEs received data, and we inserted a 15 s time interval between the two transmissions.

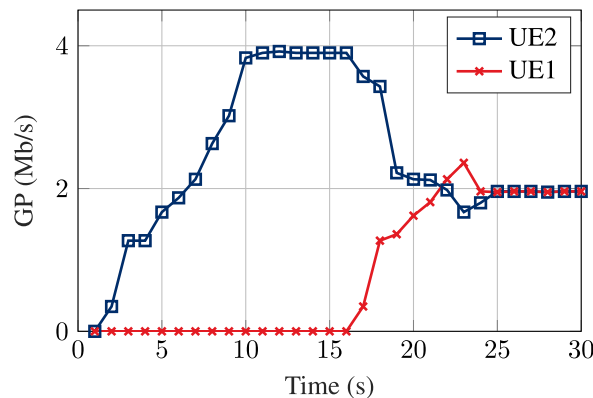


FIGURE 11. Transmission control protocol (TCP) goodput measurement with two UEs in the downlink (UE1 is starting after 15 s; single TCP stream). TCP slow start uses a low bitrate to start. Due to the round-trip delay, the goodput slowly increases to the available bandwidth. Subsequently, both UEs share the resources.

Figures 11 and 12 depict the TCP GPs of the two users concurrently. When both users are active, the resources are divided, ensuring equal GPs for both. Notably, the slow-start mechanism of TCP affects the resource distribution of the two UEs connected over the GEO satellite.

E. VALIDATION OF APPLICATIONS

On the basis of the in-lab performance analysis method in [8], we evaluated several applications over the satellite. Our user manual is available as a pdf document [23]. The results show that the testbed can be used to evaluate different use cases over a 3GPP 5G-NR based satellite network.

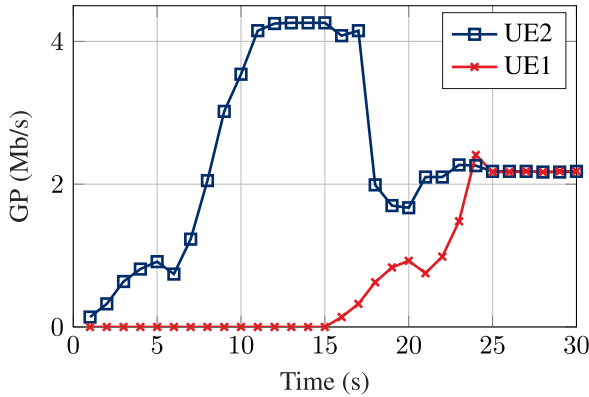


FIGURE 12. Transmission control protocol (TCP) goodput measurement with two UEs in the uplink (UE1 is starting after 15 s; single TCP stream). TCP slow start uses a low bitrate to start. Due to the round-trip delay, the goodput slowly increases to the available bandwidth. Subsequently, both UEs share the resources.

1) VOICE OVER IP

We conducted a test using a *SIPp*³-based VoIP call that transmitted audio data via real-time transport protocol (RTP) from the UE to the 5GC. We captured the RTP traffic via *Wireshark* and extracted the audio file for comparison with the original file to calculate the mean opinion score (MOS) via the *ViSQOL*⁴ tool (Figure 13). The computed MOS confirmed the excellent quality of the audio and proved that the 5G-NTN testbed could handle the continuous RTP-based network traffic without significant loss. However, the demonstration indicated that an increase in the number of VoIP sessions resulted in a decrease in audio quality.

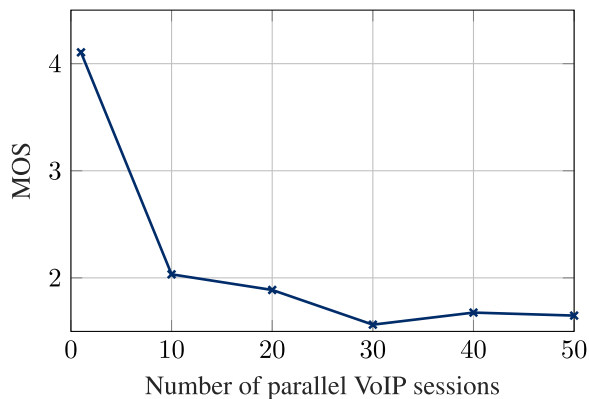


FIGURE 13. Mean opinion score values of parallel voice over IP sessions. The quality decreases as the number of parallel sessions increases.

2) WEB BROWSING

To evaluate the performance of our 5G-NTN testbed for web browsing, we utilized *Browsertime*⁵ software. This

³<https://github.com/SIPp/sipp/releases/tag/v3.6.1>

⁴<https://github.com/google/visqol/releases/tag/v3.3.3>

⁵<https://github.com/sitespeedio/browsertime/releases/tag/v16.8.0>

tool allowed us to collect performance metrics while loading several websites [24] with cached and uncached content. We chose two metrics to measure the browsing experience. The primary metric was the page load time (PLT), which measures the time it takes for a website to load, from initiation to completion in the browser. The secondary metric was the first contentful paint (FCP), which measures the time it takes for the browser to render the first bit of content after navigating to a website. Each selected website was loaded five times to ensure accurate results.

Figure 14 shows that the ideal PLT was between 0 s to 3 s for uncached web pages utilizing the terrestrial fiber connection of the University of the Bundeswehr Munich. The PLT value increased when we executed our web browsing measurements over the GEO satellite link. The FCP and PLT performance can be significantly improved if we load webpages a second time with content in the browser cache. The PLT we measured is comparable to downloading a small website via a commercial GEO satellite internet provider [21].

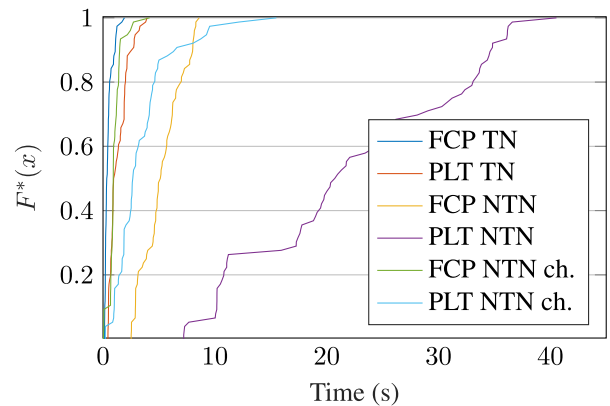


FIGURE 14. Empirical cumulative distribution function $F^*(x)$ is the probability that the loading time is smaller or equal to the abscissa. Cached web browsing content reduced the first contentful paint (FCP) and page load time (PLT) metrics of our 5G-NTN testbed.

3) INTERNET SPEED TEST

We conducted 15 Ookla speed tests from the UE to an internet server to compare the measured GP and latency. The average results displayed in Table 7 confirm our previous results regarding UL and DL GP. However, we noted a greater latency than in the initial measurements with the ping command. This was due mainly to the additional internet connection needed to connect our lab to the Ookla server.

TABLE 7. Ooklas internet speedtest results.

Uplink (Mb/s)	Downlink (Mb/s)	Latency (ms)
4.11	3.61	549

4) YOUTUBE VIDEO STREAMING

Table 8 shows the results of our YouTube live video streaming tests for videos with 720p resolution using *YouTube statistics for Nerds*. We took a snapshot of the live YouTube video after 10000 frames. Our findings indicate that the OAI 5G-NTN prototype provides reliable communication with minimal disruption in video quality. The results show that the 5G-NTN testbed can support HTTP-based live streaming use cases with a maximum video resolution of 720p.

TABLE 8. Snapshot of the measurement results of live video streaming for the 5G-NTN demonstrator.

Dropped Frames	No. of Measurement Frames	Connection Speed (kb/s)	Buffer Health (s)
6	10289	2766	3.37

VI. FUTURE WORK

The main focus of our work on the 5G-GOA testbed was on the user plane, specifically on implementing RAN1 and RAN2 improvements. Our implementation guarantees the establishment of a PDU session after the initial synchronization and RA process. For our prototype, we consider a GEO satellite link with a wide beam, eliminating the need for mobility procedures. However, we still need to implement several additional features to ensure compliance with 3GPP mobility enhancements for 5G-NTNs.

During our project, we addressed a number of challenges. For example, we disabled the HARQ process in OAI to avoid “HARQ stalling.” 3GPP suggests increasing the number of HARQ processes from 16 to 32 for LEO satellites and disabling HARQ feedback for GEO satellites. We did not fully consider this recommendation, so we did not switch off the HARQ feedback at the RLC layer in a dynamic way for every HARQ process.

While our compliance with the TA value calculation is only partial, we contribute to the first tests of 3GPP-based 5G-NTNs. According to 3GPP, the gNB should compute the common part of the TA for the feeder link and transmit it to the UEs through PBCH (SIB19). The UE should compute the UE-specific part of the TA via its GNSS-based position and satellite trajectory data. Our UE did not have GNSS capabilities, and our gNB did not receive live satellite trajectories for computing the feeder link delay, so we did not fully comply with these recommendations. 3GPP considers a UE with GNSS capabilities in their RAN2 working group and a SIB19 broadcast to receive the satellite position information (ephemeris data). Our OAI modification did not consider this enhancement because we estimated the initial TA value with a proprietary OAI function in the *phy-test mode*. In addition, we did not consider tracking area management or idle/connected mode mobility enhancements for our system scenario with a large beam.

The RAN3 working group has proposed various improvements for the 5G-NTN, primarily aimed at LEO satellites and situations involving frequent user movement. Xn handover procedures, for example, allow a conditional handover process between two gNBs. However, our work deals with a relatively static scenario in which handover is unnecessary. We present a summary of improvements to be made in future work in Table 9.

TABLE 9. Additional 3GPP release 17 5G-NTN enhancements.

Working Group	Impact
RAN1: Physical layer	Improvements to the hybrid automatic repeat request process (e.g., disabling of feedback messages)
RAN2: Access layer	Control plane: Tracking area management Idle/connected mode UE location services System information broadcast
RAN3: Access Network Architecture	Feeder link switch for LEO satellites Registration update and paging Network identity handling Cell relation handling Operations, administration, and maintenance

VII. CONCLUSION

Open research platforms that allow live demonstrations of the 5G-NTN standard are essential for supporting the applied research of publicly funded research institutions. We closely monitored the 5G-NTN work items of 3GPP Release 17 and made necessary changes to the OAI software. Our features enable long round-trip times to be handled by compensating within different 5G-NR protocol stack layers. This paper summarizes the results of the end-to-end evaluation of our 5G-NTN implementations over a GEO satellite. Our results show that our testbed can handle the varying delays of a GEO satellite and allows the UE to perform the initial attachment. In addition, we achieve the expected UL and DL throughput. Typical end-user applications such as VoIP, video streaming, and web browsing are demonstrated via our testbed. Our findings suggest that our open-source software solution is suitable for setting up 5G-NTN testbeds with up to two UEs and one gNB, including 5GC. The mobility aspects of satellites were not considered further in this paper and will, therefore, be part of future implementations in OAI.

ACKNOWLEDGMENT

The views expressed herein do not reflect the official opinion of European Space Agency.

REFERENCES

- [1] “Study on new radio (NR) to support non-terrestrial networks (release 15) v15.3.0,” 3GPP, Tech. Rep. 38.811, Jul. 2020.
- [2] *Technical Specification Group Radio Access Network; Solutions for NR to Support Non-Terrestrial Networks (NTN) (Release 16)*, document TR 38.821, 3GPP, Dec. 2019.

- [3] M. El Jaafari, N. Chuberre, S. Anjuere, and L. Combelles, "Introduction to the 3GPP-defined NTN standard: A comprehensive view on the 3GPP work on NTN," *Int. J. Satell. Commun. Netw.*, vol. 41, no. 3, pp. 220–238, May 2023.
- [4] A. Vanelli-Coralli, N. Chuberre, G. Masini, A. Guidotti, and M. E. Jaafari, *5G Non-Terrestrial Networks: Technologies, Standards, and System Design*. Hoboken, NJ, USA: Wiley, 2024.
- [5] S. Kumar, A. K. Meshram, A. Astro, J. Querol, T. Schlichter, G. Casati, T. Heyn, F. Völk, R. T. Schwarz, A. Knopp, P. Marques, L. Pereira, R. Magueta, A. Kapovits, and F. Kaltenberger, "OpenAirInterface as a platform for 5G-NTN research and experimentation," in *Proc. IEEE Future Netw. World Forum (FNWF)*, Oct. 2022, pp. 500–506.
- [6] 5G GOA Consortium. (May 2021). *5g-goa-5g Enabled Ground Segment Technologies Over the Air Demonstrator*. [Online]. Available: <https://artes.esa.int/projects/5ggoa>
- [7] F. Kaltenberger, A. P. Silva, A. Gosain, L. Wang, and T.-T. Nguyen, "Open AirInterface: Democratizing innovation in the 5G era," *Comput. Netw.*, vol. 176, Jul. 2020, Art. no. 107284.
- [8] F. Völk, R. T. Schwarz, and A. Knopp, "In-lab performance analysis of a 5G non-terrestrial network using OpenAirInterface," in *Proc. IEEE Int. Conf. Wireless Space Extreme Environments (WiSEE)*, Sep. 2023, pp. 167–172.
- [9] F. Völk, T. Schlichter, F. Kaltenberger, T. Heyn, G. Casati, R. T. Schwarz, and A. Knopp, "Field trial of a 5G non-terrestrial network using OpenAirInterface," *IEEE Open J. Veh. Technol.*, vol. 3, pp. 243–250, 2022.
- [10] 5G GOA Consortium. (2022). *Openairinterface 5g-ntn Commit*. [Online]. Available: <https://gitlab.eurecom.fr/oi/openairinterface5g/-tree/goa-5g-ntn>
- [11] A. Vanelli-Coralli, A. Guidotti, T. Foggi, G. Colavolpe, and G. Montorsi, "5G and beyond 5G non-terrestrial networks: Trends and research challenges," in *Proc. IEEE 3rd 5G World Forum (5GWF)*, Sep. 2020, pp. 163–169.
- [12] H. Määttä, J. Sedin, S. Parolari, and R. S. Karlsson, "Radio interface protocols and radio resource management procedures for 5G new radio non-terrestrial networks," *Int. J. Satell. Commun. Netw.*, vol. 41, no. 3, pp. 276–288, May 2023.
- [13] S. Ahmadi, *5G NR: Architecture, Technology, Implementation, and Operation of 3GPP New Radio Standards*. New York, NY, USA: Academic, 2019.
- [14] Ericsson. (2023). *Using 3gpp Technology for Satellite Communication*. [Online]. Available: <https://www.ericsson.com/en/reports-and-papers/ericsson-technology-review/articles/3gpp-satellite-communication>
- [15] S. Kumar, C. K. Sheemar, J. Querol, A. Nik, and S. Chazinotas, "Experimental study of the effects of RLC modes for 5G-NTN applications using OpenAirInterface5G," in *Proc. IEEE Globecom Workshops (GC Wkshps)*, vol. 2021, Dec. 2023, pp. 233–238.
- [16] S. Cioni, X. Lin, B. Chamailard, M. E. Jaafari, G. Charbit, and L. Raschkowski, "Physical layer enhancements in 5G-NR for direct access via satellite systems," *Int. J. Satell. Commun. Netw.*, vol. 41, no. 3, pp. 262–275, May 2023.
- [17] *Nr; Packet Data Convergence Protocol (pdcp) Specification*, document 38.323, 3GPP, 2022.
- [18] *Nr; Radio Link Control (rlc) Protocol Specification*, document 38.322, 3GPP, 2023.
- [19] *Nr; User Equipment (ue) Radio Access Capabilities*, document 38.306, 3GPP, 2023.
- [20] D. Racelis and M. Joerger, "High-integrity TLE error models for MEO and GEO satellites," in *Proc. AIAA SPACE Astronaut. Forum Exposit.*, Sep. 2018, p. 5241.
- [21] J. Deutschmann, K. S. Hielscher, and R. German, "Satellite internet performance measurements," in *Proc. 2019 Int. Conf. Networked Syst.*, 2019, pp. 2019–2022.
- [22] J. Deutschmann, S. Jahandar, K.-S. Hielscher, and R. German, "Internet via satellite: GEO vs. LEO, OpenVPN vs. Wireguard, and CUBIC vs. BBR," in *Proc. 1st ACM MobiCom Workshop Satell. Netw. Comput.*, Oct. 2023, pp. 19–24.
- [23] F. Völk. *User Manual on How To Use the Apps for Performance Evaluation*. Accessed: Oct. 22, 2024. [Online]. Available: https://drive.google.com/open?id=1Cvq5AGfv6LUWnfFlkOtLkfUONMFjtWGR&usp=drive_copy
- [24] F. Völk. *21 Selected Websites for Web-browsing Evaluation Based on Amazon Alexa Top Sites*. Accessed: Oct. 22, 2024. [Online]. Available: https://drive.google.com/file/d/1RkvpGLxQxVGZPPMsPNay14LYhUjXvWck/view?usp=drive_link



FLORIAN VÖLK (Graduate Student Member, IEEE) received the master's degree in electrical engineering and information technology in Nuremberg and Melbourne, in 2016, with a focus on communications engineering. He is currently pursuing the Ph.D. degree with the University of the Bundeswehr Munich. Since 2016, he has been a Research Fellow with the University of the Bundeswehr Munich. His research interests include physical layer techniques, system design, and architecture optimization for integrated satellite-terrestrial networks. In addition, he has a strong interest in prototyping, experimental work, and testbeds.



THOMAS SCHLICHTER received the Dipl.-Inf. degree in computer engineering from the University of Mannheim, Germany, in December 2003. From 2004 to 2009, he was a Research Assistant with the Department of Hardware-Software Co-Design, University of Erlangen-Nuremberg, Germany. In 2009, he joined the Fraunhofer Institute for Integrated Circuits (IIS). He has conducted design and implementation of hardware-software interfaces and high-speed FPGA hardware for ESA and EU projects, as well as supervising student work on different topics, such as software-defined radio and high-level synthesis. As a Senior Engineer, he contributed to the ESA SATINET Project on LTE backhauling over satellites, the ESA Project SCORSESE on distributing multimedia content via satellite-aided terrestrial networks, the ESA Project SATiS5 on satellite integration in 5G networks, and the 5G-GOA and 5G-LEO for 5G-NR NTN direct access via GEO and LEO satellites. In addition to contributing software to the Open Air Interface RAN Project, he is a member of the Open Air Interface Software Alliance (OSA) Technical Committee.



SUMIT KUMAR (Member, IEEE) received the B.Tech. degree in electronics and communication engineering from Gurukula Kangri University, Haridwar, India, in 2008, the M.S. degree in wireless communication and signal processing from the International Institute of Information Technology, Hyderabad, India, in 2014, and the Ph.D. degree in wireless communication from Eurecom, France, in 2019. During the master's degree, he was involved in several projects funded by the Department of Science and Technology, India. His Ph.D. thesis focused on interference management and the coexistence of wireless systems and the architecture for a multistandard SDR receiver was developed and demonstrated. In 2019, he joined the SIGCOM Research Group, Interdisciplinary Centre for Security, Reliability, and Trust (SnT), University of Luxembourg, Luxembourg, as a Research Associate. He is involved in several European Space Agency (ESA) and Luxembourgish national projects related to 5G, 5G non-terrestrial networks, EMF radiation, and satellite communication. His research interests include software defined radio, interference management, 5G, 5G-NTNs, and computer networking.



ROBERT T. SCHWARZ (Member, IEEE) received the Ph.D. degree (Hons.) in satellite communications from the University of the Bundeswehr Munich, in 2019. From 2006 to 2012, he was with the Federal Office, Bundeswehr for Information Management and Information Technology, where he was involved in German Program for Satellite Communications of the Bundeswehr (SAT-COMBw). Since 2012, he has been a Research Fellow with the University of the Bundeswehr Munich. His research interests include digital signal processing, waveform design, and MIMO for satellites and other non-terrestrial networks. He is a member of German Engineers' Association, VDE/ITG, and AFCEA.



ANDREAS KNOPP (Senior Member, IEEE) received the Ph.D. degree (Hons.) in radio communications from University of the Bundeswehr Munich, in 2008. Since 2014, he has been a Full Professor of signal processing and has also coordinated the Munich Center for Space Communications, which is Germany's largest SpaceCom Laboratory and Experimental Satellite Ground Station. Before taking up a faculty position, he gained expertise as a Communications Engineer and the Satellite Program Manager. His current research interests include satellite network integration and waveform design for 6G, digital satellite payloads, secure/antijam communications, and low-power mMTC. He is an Entrepreneur and the Co-Founder of two start-up companies that have implemented his research. He is an advisor to German MoD and a member of the Expert Group on Radio Systems, German Engineers' Association, and VDE/ITG and AFCEA.



MARWAN HAMMOUDA received the Ph.D. degree in electrical engineering from the Gottfried Wilhelm Leibniz Universität, Hanover, in 2019. In his thesis, he focused on investigating the performance of different 5G technologies (e.g., massive MIMO and nonorthogonal multiple access). Shortly after that, he joined Smart Microwave Sensors GmbH, a company specializing in automotive radar systems, where he was a Signal Processing Engineer to develop and implement different signal processing algorithms for automotive radar systems. He then joined Fraunhofer IIS, as a Research Associate, in 2022. He has been involved in ESA projects 5G-GOA and 5G-LEO to enable direct 5G connectivity over GEO and LEO satellites, respectively. His current research interests include future mobile networks (5G and beyond) with a focus on satellite networks in 5G.



THOMAS HEYN received the Dipl.-Ing degree in electrical engineering from Friedrich-Alexander University, Erlangen, in 1996. He joined Fraunhofer IIS shortly thereafter. He is currently the Head of the Connectivity Group, Broadcast and Broadband Department, and is a member of the network2020 European Technology Platform. His current research interests include future mobile networks and investigating the evolution of 4G and 5G technologies, such as virtual-MIMO concepts, high-speed front-/backhauling, convergence of broadcast and broadband, and satellite/terrestrial networks in 5G. As a 3GPP delegate for Fraunhofer IIS, since 2015, he has been one of the first in 3GPP to integrate NTN and satellites into a new mobile communications standard. Currently, he and his team pursue this goal for RAN1 and RAN3. Owing to his years of satellite experience, he is responsible for satellite standardization efforts in 3GPP in the ESA project ALIX. Furthermore, he was one of the initial driving forces behind Fraunhofer joining the Open Air Interface Software Alliance. For 5G-LEO, he will continue to monitor 3GPP standardization for the 5G-NTN, especially in Release 17 and the start of Release 18, and will act as an advisor for operational scenarios, the system architecture, and the selection of the necessary NR features, which will be implemented specifically for NTNs in the 5G-LEO testbed.



JORGE QUEROL (Member, IEEE) was born in Forcall, Castelló, Spain, in 1987. He received the B.Sc. degree in telecommunication engineering, the M.Sc. degree in electronics engineering, the M.Sc. degree in photonics, and the Ph.D. degree (cum laude) in signal processing and communications from the Universitat Politècnica de Catalunya-BarcelonaTech (UPC), Barcelona, Spain, in 2011, 2012, 2013, and 2018, respectively. His Ph.D. thesis focused on the development of novel antijamming and counterinterference systems for global navigation satellite systems (GNSSs), GNSS reflectometry, and microwave radiometry.

One of his outstanding achievements was the development of a real-time standalone precorrelation mitigation system for GNSSs named FENIX, which was applied on a customized software-defined radio (SDR) platform. FENIX was patented, licensed, and commercialized by MITIC Solutions, a UPC spin-off company. In 2018, he joined the SIGCOM Research Group, Interdisciplinary Centre for Security, Reliability, and Trust (SnT), University of Luxembourg, Luxembourg, as a Research Associate, and was promoted to a Research Scientist, in 2021. He is currently the Head of the SatComLab/5G-SpaceLab. He is involved in several ESA and Luxembourgish national research projects dealing with signal processing, satellite and space communications, signal processing, and satellite navigation. His research interests include software-defined radios (SDRs), real-time signal processing, satellite communications, 5G non-terrestrial networks, satellite navigation, and remote sensing. He received the Best Academic Record Award of the Year in Electronics Engineering at UPC in 2012, the First Prize of European Satellite Navigation Competition (ESNC) Barcelona Challenge from European GNSS Agency (GSA) in 2015, the Best Innovative Project of the Market Assessment Program (MAP) of the EADA Business School in 2016, the Isabel P. Trabal Award from Fundació Caixa d'Enginyers for quality research during the Ph.D. degree in 2017, and the Best Ph.D. Thesis Award in remote sensing in Spain from the IEEE Geoscience and Remote Sensing (GRSS) Spanish Chapter in 2019.



SYMEON CHATZINOTAS (Fellow, IEEE) is currently a Full Professor/Chief Scientist and the Head of the SIGCOM Research Group, SnT, University of Luxembourg. He is coordinating research activities on communications and networking, acting as a PI for more than 20 projects, and is the main representative for 3GPP, ETSI, and DVB. He was previously a Visiting Professor with the University of Parma, Italy, lecturing on 5G wireless networks. He was involved in numerous research and development projects for NCSR Demokritos, CERTH Hellas and CCSR, and the University of Surrey. He has co-authored more than 450 technical papers in refereed international journals, conferences, and scientific books. He was a co-recipient of the 2014 IEEE Distinguished Contributions to Satellite Communications Award and the Best Paper Awards at EURASIP JWCN, CROWCOM, and ICSSC. He is on the Editorial Board of IEEE TRANSACTIONS ON COMMUNICATIONS, the IEEE OPEN JOURNAL OF VEHICULAR TECHNOLOGY, and the *International Journal of Satellite Communications and Networking*.



ADAM KAPOVITS was born in Budapest, Hungary, in April 1965. He received the degree in electrical engineering from Budapest University of Technology and Economics, in 1989. He was with Hungarian Telecom MATÁV (currently Magyar Telekom), from 1990 to 1999, initially as a part of an expert team supporting the build-out of the national fiber optic network, but later was responsible for all European research and development collaborations by MATÁV. He joined Eurescom GmbH, the leading European provider of management and support services in high-tech areas, with a focus on information and communications technologies, in 1999. He holds the position of the Programme Manager of Eurescom and is responsible for the preparation and management of Horizon Europe research projects of European Union and the management of research projects contracted by European Space Agency. He acted as the Project Lead for more than ten ESA research projects with Eurescom. All of these ESA research projects focused on the convergence of terrestrial mobile communication and satellite communication.

...